Title
Heavy Residue Spectra in the Interaction of 85 A MeV 12C with 197Au

Journal
Nuclear Physics A, 499(3)

Authors
Aleklett, K.
Johansson, M.
Lihver, L.
et al.

Publication Date
1988-12-01

LBL-26668
Preprint

Lawrence Berkeley Laboratory
UNIVERSITY OF CALIFORNIA

Submitted to Nuclear Physics A

Heavy Residue Spectra in the Interaction of 85 A MeV ^{12}C with ^{197}Au

K. Aleklett, M. Johansson, L. Sihver, W. Loveland,
H. Groening, P.L. McGaughey, and G.T. Seaborg

December 1988

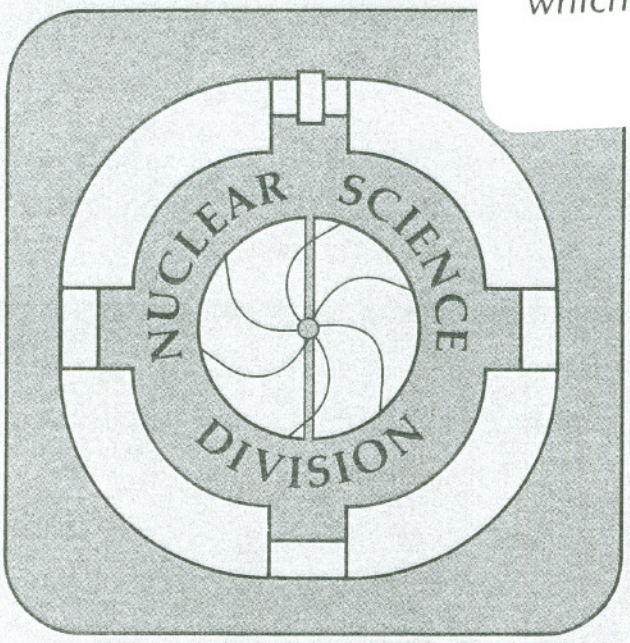

Prepared for the U.S. Department of Energy under Contract Number DE-AC03-76SF00098.

LBL-26668

HEAVY RESIDUE SPECTRA IN THE INTERACTION OF 85 A MeV ^{12}C WITH ^{197}Au

K. Aleklett, M. Johansson, and L. Sihver
University of Uppsala
The Studsvik Neutron Research Laboratory
S-611 82 Nyköping, Sweden

W. Loveland and H. Groening*
Dept. of Chemistry
Oregon State University
Corvallis, OR 97331, USA

P.L. McGaughey** and G.T. Seaborg
Nuclear Science Division
Lawrence Berkeley Laboratory
Berkeley, CA 94720, USA

December 1988

This work was supported by the Director, Office of Energy Research, Office of High Energy and Nuclear Physics, Nuclear Physics Division and by the U.S. Department of Energy under Grant No. DE-FG06-88ER40402 and DE-AC03-76SF00098, and the Swedish Natural Science Research Council.

HEAVY RESIDUE SPECTRA IN THE INTERACTION OF 85 A MeV ^{12}C WITH ^{197}Au

K. Aleklett, M. Johansson, and L. Sihver
University of Uppsala
The Studsvik Neutron Research Laboratory
S-611 82 Nyköping, Sweden

W. Loveland and H. Groening*
Dept. of Chemistry
Oregon State University
Corvallis, OR 97331, USA

P.L. McGaughey** and G.T. Seaborg
Nuclear Science Division
Lawrence Berkeley Laboratory
Berkeley, CA 94720, USA

Abstract

We have measured the heavy residue differential range distributions in the interaction of 85 MeV/nucleon ^{12}C with ^{197}Au. The range distributions were converted to energy spectra using known range-energy relationships. The mean residue energies range from 15 keV/nucleon (A=189) to 314 keV/nucleon (A=131). Longitudinal momenta of the heavy residues have been deduced ($\langle p_{||} \rangle / p_{cn} = 0.27$). The mean spectral energies and the shapes of the residue spectra are shown to be in agreement with the predictions of the VUU model.

NUCLEAR REACTIONS $^{197}Au(^{12}C,X)$, E = 1032 MeV; measured fragment differential ranges; deduced $d^2\sigma/d\Omega dE$ (fragment Z,A); intermediate energy heavy ions.

(Submitted to Nucl. Phys. A, December 1988)

I. Introduction

The collision of two nuclei at intermediate energies(10-100 MeV/nucleon) frequently results in the production of large, slow-moving fragments of the target nucleus. For this work, we define these fragments (or "heavy residues" as they are called) to have mass numbers, $A_{residue}$, that are greater than 2/3 the mass number of the target. To adequately understand the dynamics of intermediate energy nuclear collisions, one needs to know and understand the properties of the heavy residues produced in these collisions.

The probability of producing heavy residues in intermediate energy nuclear collisions is substantial[1-13]. For the interaction of ^{12}C with ^{197}Au we show (in Figure 1) the dependence of

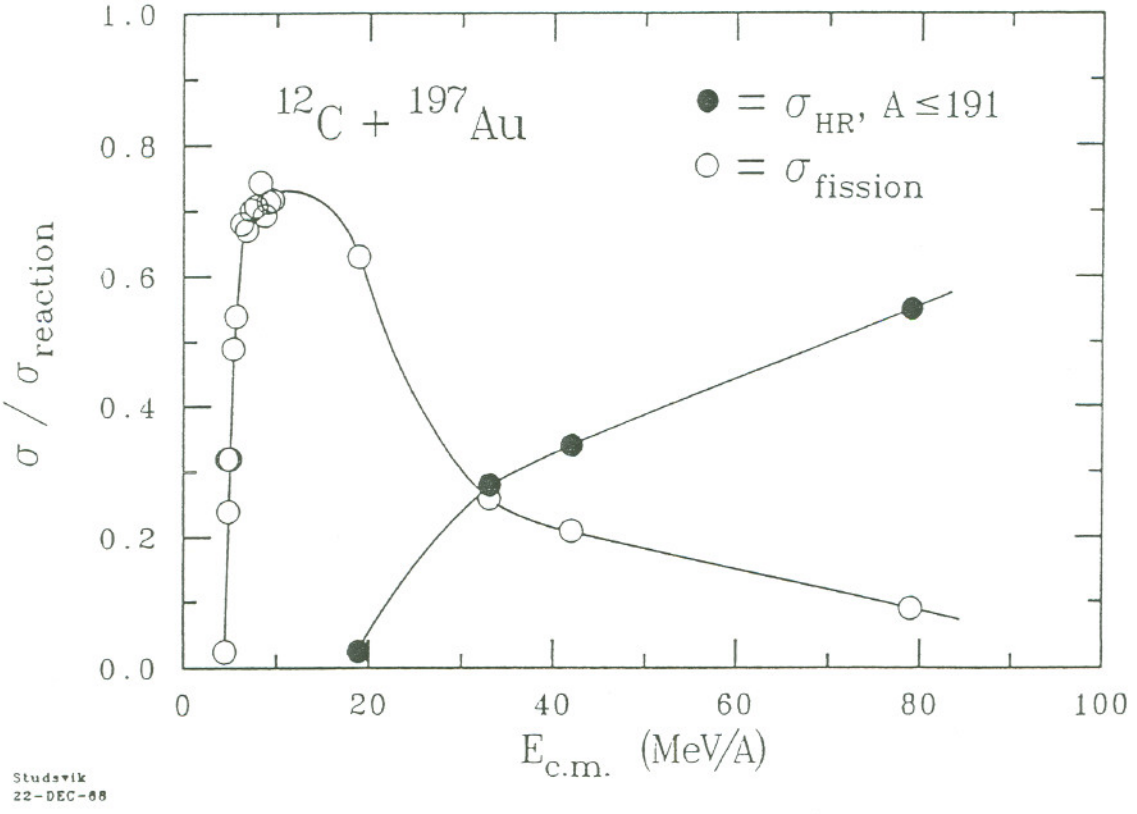

Figure 1. The dependence of the fission cross section (open circles) and the heavy residue formation cross section (solid points) on projectile energy for the interaction of ^{12}C with ^{197}Au. Data are from ref. 10, 41, 43 and 44. In integrating the mass-yield distributions we have not include yields of fragments within 5 A unit of the target A=197. These fragments are thought to have other dynamic properties then the A≤191 residues[42,44]. Consequently the σ_{HR} values are lower limits when considering all heavy residues.

cross section on projectile energy for fission and heavy residue ($A_{residue} \leq 191$) formation. One should also note that the fission fragments are primary heavy residues that de-excited by fission rather than particle emission[3,4,6]). The cross section for heavy residue production (de-excitation by particle emission) relative to the fission cross section increases with increasing projectile energy due to two effects:

(a) the faster time scale of the more energetic reactions favors the intrinsically faster process of particle emission vs. the slower collective motion of fission
(b) the increasing probability of incomplete fusion with increasing projectile energy, leading to lower mass and atomic numbers of product nuclei, thus decreasing their fissionability.

The heavy target residues can be produced in both central and peripheral collisions[4,8,9]). At low projectile energies, most residues are produced in more central collisions where they can be characterized as evaporation residues. The heavy residue angular distributions are strongly forward-peaked in all cases[4,5,6,11-14]).

Because of the large Z and A of these residues and their resulting low energies (~100 keV/nucleon), the detection of these residues is difficult. While a number of measurements of the average linear momentum transfer to the target nucleus in intermediate energy reactions have been made using the fission fragment folding angle technique, only a modest number of measurements of the energy spectra of the heavy residues have been made[11,12,13]). Lleres, et al.[11]) reported the observation of the spectra of heavy residues from the interaction of 86 MeV/nucleon ^{12}C with ^{89}Y. Their observations show single component spectra for the heaviest residues (with mean residue energies of ~100 keV/nucleon) and two-component spectra for the lighter residues ($\Delta A = A_{target} - A_{residue} > 17$). These two peaks, with mean recoil energies of ~100 keV/nucleon and 4 MeV/nucleon, are attributed to the occurrence of peripheral and central collisions, respectively. Grabez, et al.[12,13]), using CR-39 track detectors to study the reaction of 84 MeV/nucleon ^{12}C with ^{208}Pb, reported the semi-exclusive measurement of residue energy spectra. Using the track detectors to classify the type of reaction mechanism responsible for the production of a given heavy residue (by observing the type and number of associated tracks with each heavy residue track), they concluded that most heavy residues were the result of binary events producing an intermediate mass fragment ($A_{fragment} < A_{target}/3$) and a heavy residue. Most provocatively, they reported the occurrence of spallation reactions (where the heavy

residue production was accompanied only by the emission of nucleons) in which the energies of the spallation products were unusually high (~1 MeV/nucleon) and the residues were emitted sidewise to the incident projectile beam. We do not understand these reported energies and angular distributions of the spallation products which are unlike those seen in any other studies of nucleus-nucleus collisions.

We made detailed measurements of the spectra of the heavy residues produced in the intermediate energy reaction, 85 MeV/nucleon ^{12}C with ^{197}Au as a function of the residue Z and A. This reaction was chosen for study because of the large number of previous experimental [8,10,14-18]) and theoretical [19-24])studies of this reaction. We observe low average residue energies (<100 keV/nucleon) and a spectral shape that indicates that a significant fraction of these residues are produced with energies so low as to preclude their detection in some previous studies that utilized non-radiochemical measurements of the residues. We present (in Section III.D) the first successful calculation (based upon the quantum statistical mechanical VUU model) of the heavy residue spectra.

A preliminary description of a portion of these data has been presented elsewhere[25]).

II. Experimental Procedures

Inclusive measurements of the target fragment differential range spectra for the interaction of 85 MeV/nucleon ^{12}C with ^{197}Au were made using radiochemical techniques. The experiments were carried out using the CERN SC synchrocyclotron. The experimental arrangements are shown in Figure 2. Two separate experiments were performed utilizing mylar and aluminum catcher foils, respectively. The mylar catcher foil stack was designed to stop fragments as energetic as fission fragments while the aluminum foil stack was designed primarily to detect the heavy residues.

In the experiment employing mylar catcher foils, ten catcher foils ranging in thickness from 0.3 to 5.1 mg/cm^2 were used. The catcher foil stack subtended laboratory system plane angles from 6.8 to 17.7 degrees with the mean fragment entrance angle relative to the normal to the foil surface being 13.0 degrees. The 85 MeV/nucleon ^{12}C beam was collimated to an area of <10 mm^2 and was aligned along the axis of the scattering chamber. The gold target was irradiated for 540 m with average beam intensity of ~3x10^{11} ions/s. Following irradiation, the

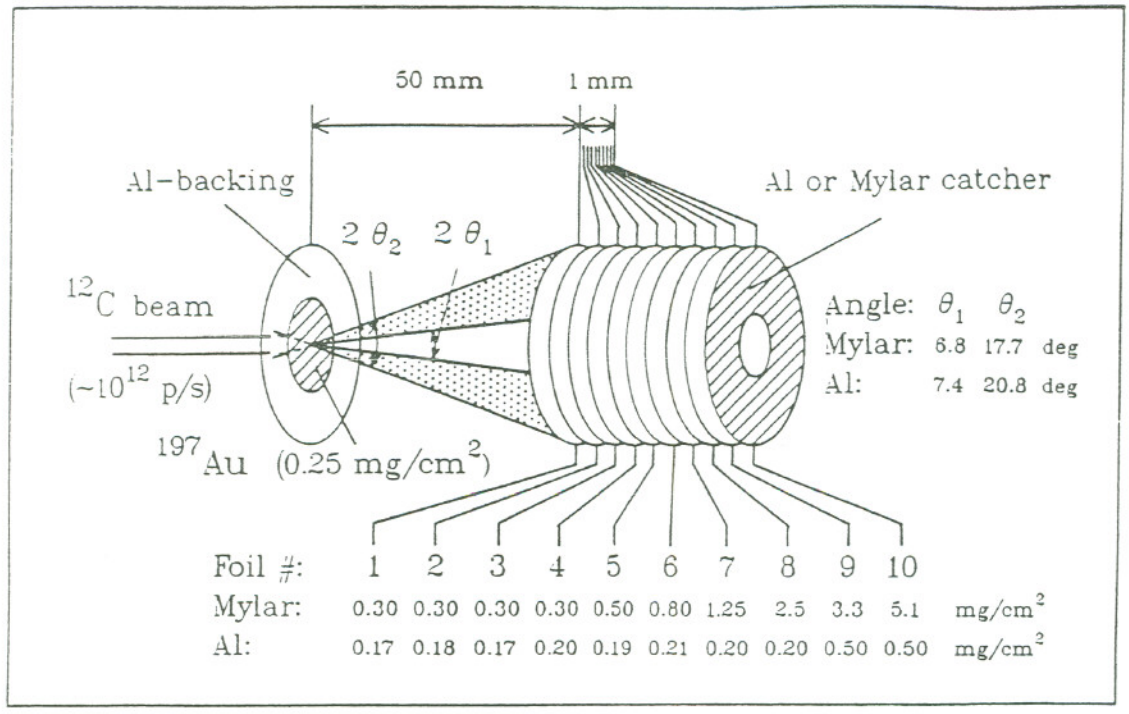

Figure 2. Schematic diagram of the experimental apparatus.

catcher foil stack was shipped to Sweden where it was disassembled and mounted for assay by off-line gamma-ray spectroscopy. Measurements began fourteen hours after the end of the irradiation.

The second experiment utilized a ten aluminum catcher foil stack with the catcher foils ranging in thickness from 0.17 to 0.50 mg/cm^2, thus enabling a higher resolution measurement for the heavy residue spectra. The catcher foil stack subtended plane angles ranging from 7.4 to 20.8 degrees, with a mean fragment entrance angle relative to the normal to the foil surface of 15.1 degrees. This experiment involved a 383 m irradiation with an average beam intensity of ~1x10^{12} ions/s. The foil assembly was disassembled immediately after irradiation and mounted for counting at CERN. After 70 hours of off-line gamma-ray spectroscopy at CERN, the foils were shipped to Sweden for further assay.

The resulting gamma-ray spectra were analyzed using the interactive analysis program DECHAOS[26]). The analysis of the decay curves and the assignment of the radionuclides present and their activities was done in a similar manner to that described previously[27]). The radioactive decay data used in these assignments was an updated form[28]) of the Reus-Westmeier tables[29]).

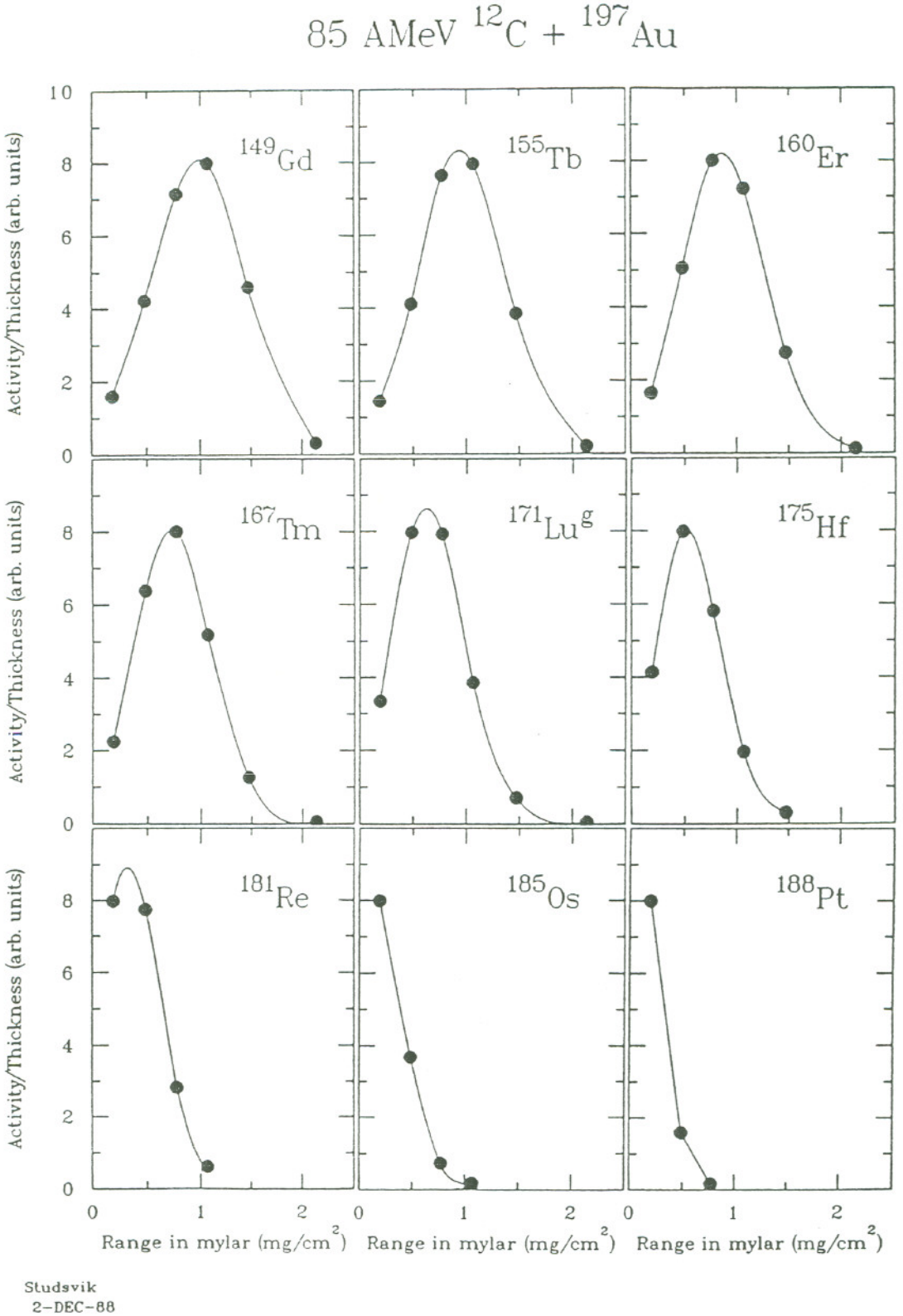

Figure 3. Heavy residue differential range distributions measured with a mylar catcher foil stack.

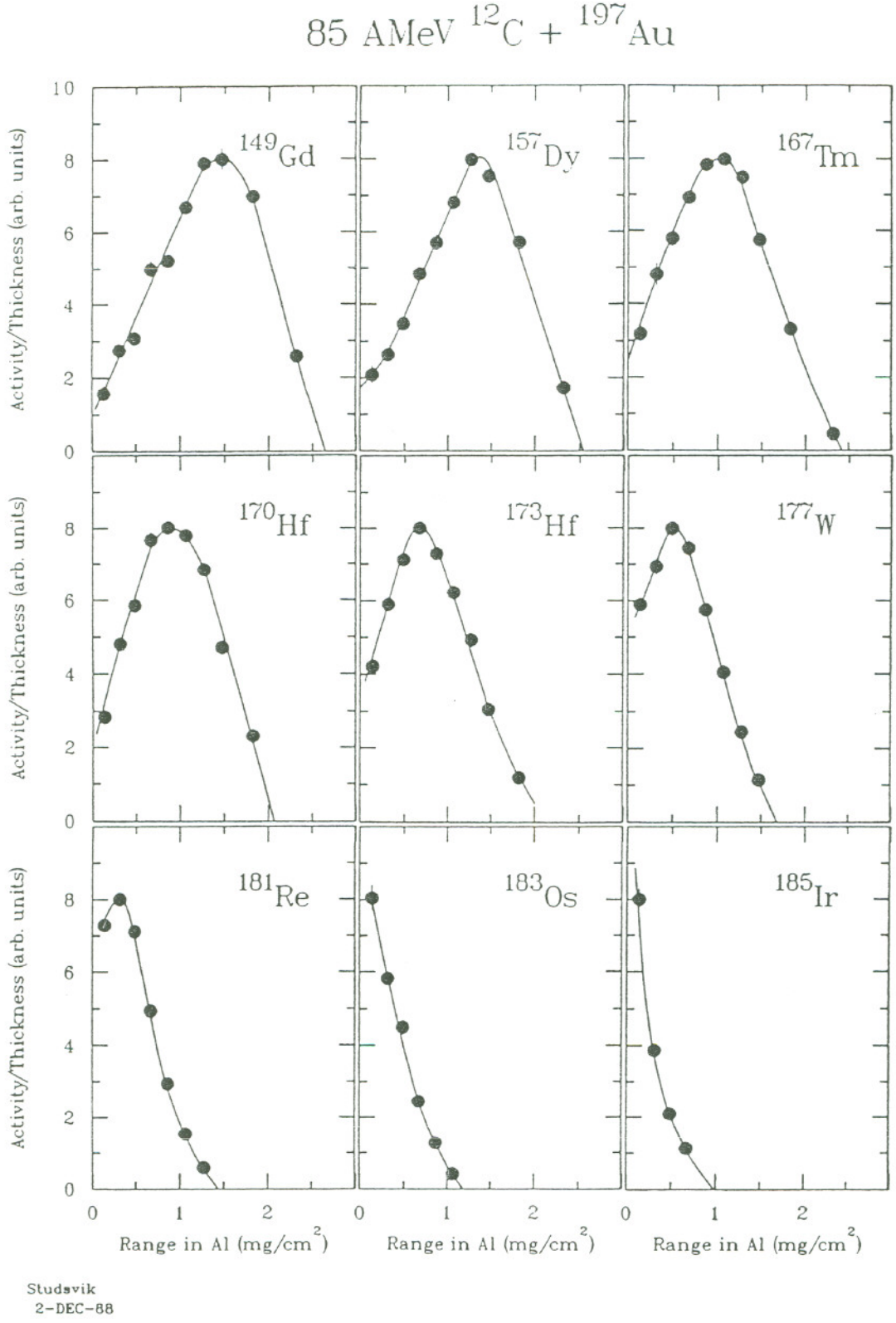

Figure 4. Heavy residue differential range distributions measured with a aluminum catcher foil stack.

From the measured activities, projected differential range distributions were calculated for the stopping of seventeen different heavy residues in mylar and eighteen different heavy residues in aluminum. A representative set of these differential range spectra is shown in figures 3 and 4. Corrections for energy loss in the gold target were made by assuming that, on the average, the fragments traversed half the effective target thickness (125 ug/cm^2). This thickness was converted to Mylar/aluminum equivalent on the basis of the relative stopping powers of gold and Mylar/aluminum[31]).

Two effects contribute to the resolution obtained in the measured range distributions, i.e., the finite, unequal thicknesses of some of the catcher foils employed and the range straggling inherent in the stopping process. (We neglect straggling due to catcher foil inhomogeneities and different path lengths in the target. Numerical simulations show the straggling introduced by the finite solid angle subtended by the catcher foils is negligible.) To help understand the type and magnitude of the effects introduced by the finite, unequal catcher foil thicknesses and range straggling, we performed a simple numerical exercise (Figure 5). We assumed a Maxwellian form for the laboratory frame heavy residue energy spectra:

$$P(E)dE = \frac{E}{T^2} \exp(-\frac{E}{T}) \qquad (1)$$

with T being the nuclear temperature. Taking as examples of typical "light" and "heavy" heavy residues, ^{149}Gd and ^{181}Re, stopping in aluminum, and assuming values of T of 12.7 and 3.90 MeV, respectively, we transformed the resulting energy spectra into range distributions using the range-energy tables of Northcliffe and Schilling[31]). The effects of range straggling upon the range distributions were calculated using the equation

$$P(R)dR = \frac{1}{R_o \rho \sqrt{2\pi}} \exp\left[-\left(\frac{R-R_o}{\sqrt{2}\, R_o \rho}\right)^2\right] \qquad (2)$$

where R_o is the average range of a monoenergetic ion, ρ is the straggling parameter and $R_o\rho$ is the range straggling. Values of the straggling parameter for the A=149 ion stopping in aluminum were taken from previous measurements of that quantity[32]) while straggling parameters for the A=181 ion were calculated from the measured values for A=149 assuming that the dependence of ρ upon ion mass is given by the LSS expression[33])

$$\rho = \left| \frac{2}{3} \cdot \frac{A_{stopper} \cdot A_{ion}}{(A_{stopper} + A_{ion})^2} \right|^{\frac{1}{2}} \qquad (3)$$

The simulations were done in energy steps of 10 keV/nucleon. The binning of the data into thicknesses of catcher foil equivalent was done after converting the ion energies to ranges in aluminum. In Figure 5 we show the range distribution corresponding to the Maxwellian energy distribution without and with straggling effects. For the more energetic fragment (A=149) the effect of range straggling seems to be negligible while the effect of binning the data into finite, unequal catcher foil equivalent thicknesses and the existence of some fragments that would "punch through" our foil stack causes some distortion. For example, the mean range calculated from the continuous Maxwellian spectrum is 1.37 mg/cm^2. Binning the data into catcher foil equivalent thicknesses and discarding those fragments that would punch through our stack gives, upon recalculation, a mean range of 1.23 mg/cm^2 (neglecting punch through gives a mean range of 1.35 mg/cm^2). Adding in the effect of straggling does not affect the calculated value of the mean range.

For the less energetic fragment (A=181), the foil thicknesses are approximately equal but there is a clear degradation of resolution in the range distribution due to the finite thickness of the first foil and the effects of range straggling. The values of the mean ranges are shifted by 4% due to these effects. In the A=149 case, the measured range distribution does not have the shape of the calculated laboratory frame Maxwellian distribution (see Section III for further discussion).

We did not attempt to unfold the effects of the range straggling or "binning" in our data. From the simulations, we conclude that (apart from the shape of the low energy portion of the range distribution for the least energetic fragments and some uncertainties in the values of the mean ranges for those fragments that were energetic enough to penetrate to the latter, very thick foils of our range stacks) that these effects could be neglected. Based upon the numerical simulations we conclude that the values of the mean fragment energies deduced from the differential range measurements are, in general, uncertain to < 10%.

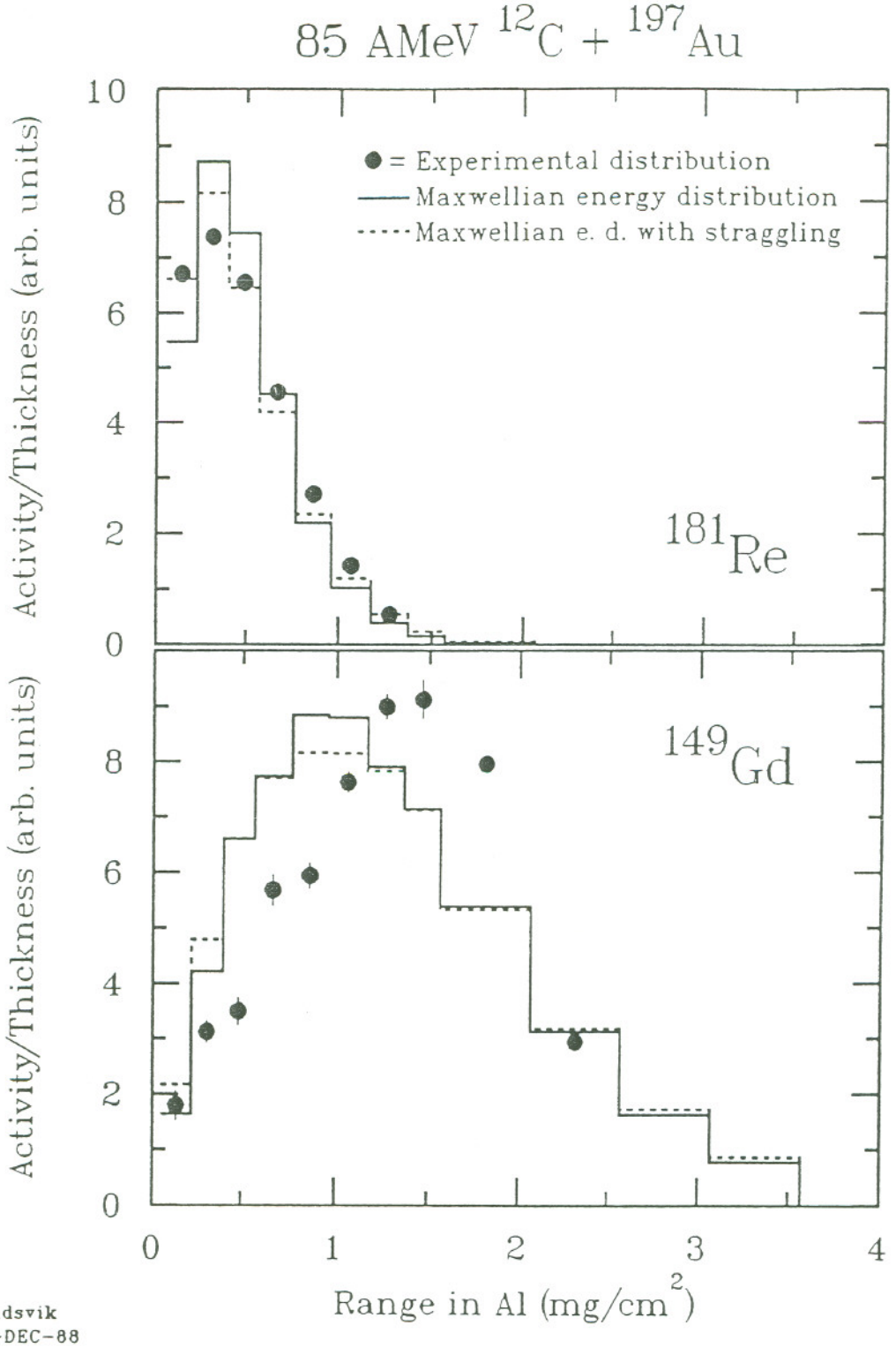

Figure 5. Numerical simulations of the effect of straggling and finite foil thickness upon the measurement of the differential range spectra of ^{149}Gd and ^{181}Re stopping in aluminum.

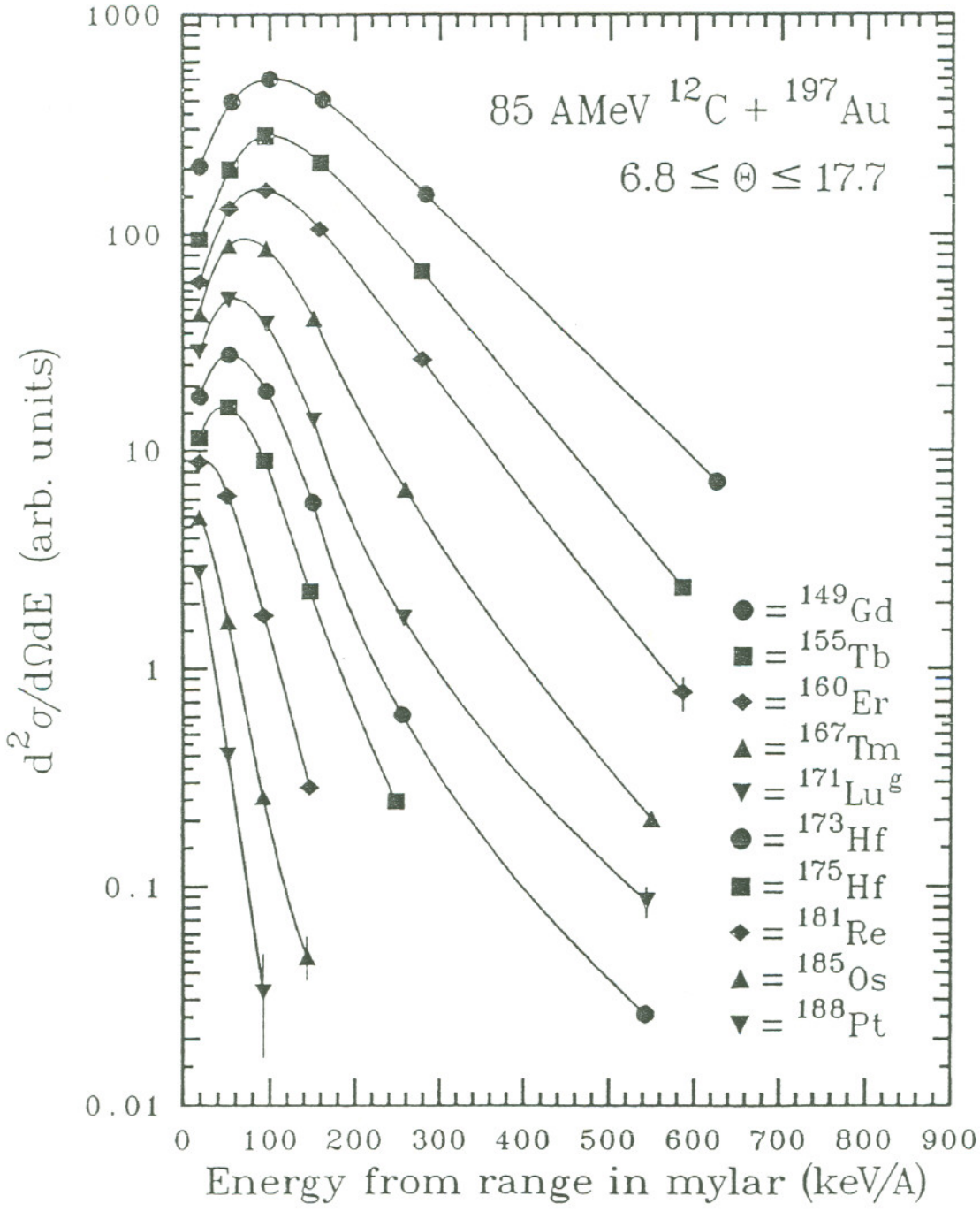

Figure 6. Heavy residue energy spectra deduced from the mylar differential range distributions.

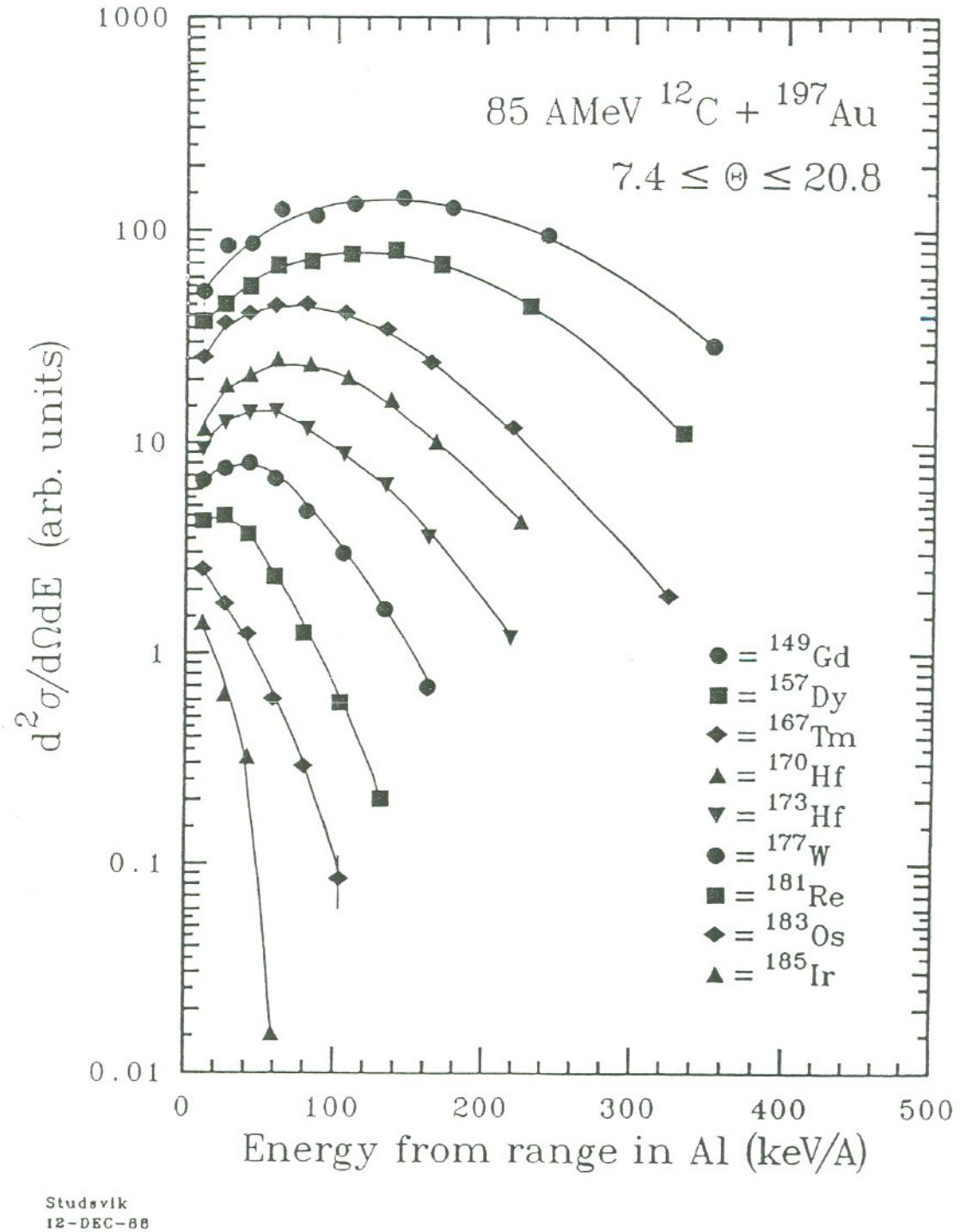

Figure 7. Heavy residue energy spectra deduced from the aluminum differential range distributions.

III. Results and Discussion

A. Comparison of mylar and aluminum catcher foil data

The differential range distributions shown in Figures 3 and 4 were transformed into energy spectra using the range-energy relations of Northcliffe and Schilling[31]). The resulting spectra are shown in Figures 6 and 7. The mean fragment ranges and energies deduced from the measurements using mylar and aluminum catcher foils are given in in Table 1. There is good general agreement between the mean energies deduced in each case (Figure 8), giving confidence in the internal consistency of the range-energy relationships used. In Figure 9, we compare the deduced fragment energy spectra for a typical heavy residue, ^{167}Tm, as deduced from our measurements with mylar and aluminum catcher foils. Apart from the poorer resolution of the mylar "detector stack", the two spectra are similar. There is some indication of greater straggling, i.e., a larger number of low and high energy events in the

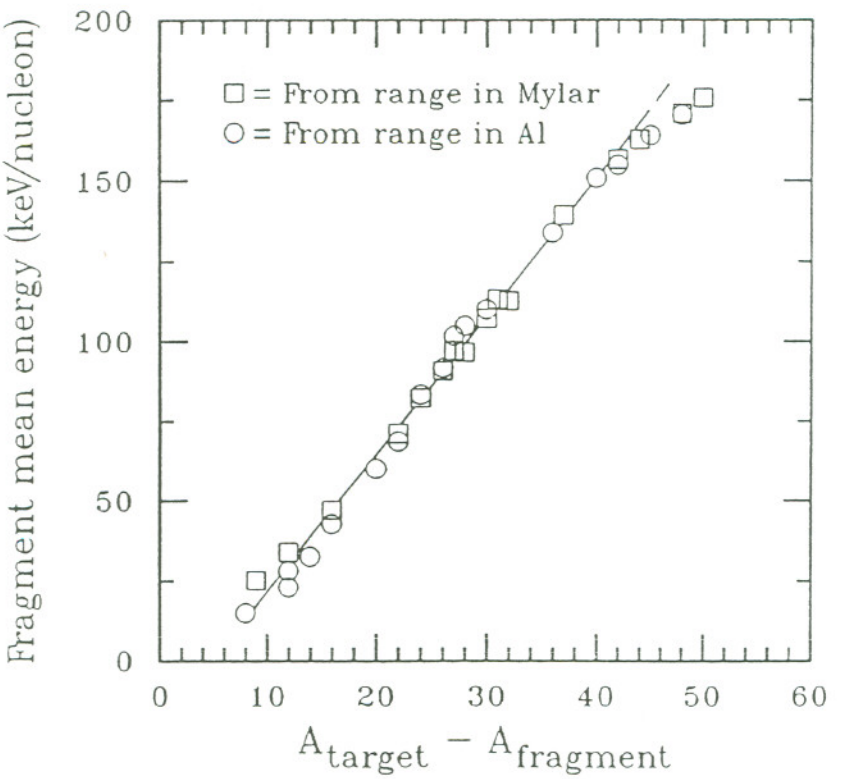

Figure 8. Mean heavy residue energies as a function of the difference between the residue mass number and the target mass number. The solid line ($E=4.29*\Delta A-21.3$ keV/nucleon; $8 \leq \Delta A \leq 45$) represents an empirical representation of the data in which the fragment energy is taken as a linear function of ΔA.

Table 1: Mean fragment ranges and energies for residues produced in the interaction of 85 A MeV ^{12}C with ^{197}Au. The measurements were performed using aluminum and Mylar catcher foils.

Nuclid	ΔA[1]	<Range Al> (mg/cm^2)	<Range Mylar> (mg/cm^2)	<Energy (Al)>[2] (keV/nucleon)	<E. (Mylar)>[2] (keV/nucleon)
^{189}Pt	8	0.189 +/- 0.007		15.1 +/- 0.6	
^{188}Pt	9		0.248 +/- 0.008		25.3 +/- 1.0
^{185}Ir	12	0.277 +/- 0.010		23.1 +/- 0.8	
^{185}Os	12	0.339 +/- 0.010	0.321 +/- 0.006	28.3 +/- 0.9	34.1 +/- 0.7
^{183}Os	14	0.381 +/- 0.013		32.7 +/- 1.2	
^{181}Re	16	0.486 +/- 0.007	0.421 +/- 0.006	42.8 +/- 0.6	47.1 +/- 0.7
^{177}W	20	0.646 +/- 0.012		60.3 +/- 1.2	
^{175}Hf	22	0.725 +/- 0.019	0.588 +/- 0.004	68.8 +/- 1.9	71.3 +/- 0.6
^{173}Hf	24	0.838 +/- 0.007	0.643 +/- 0.006	83.4 +/- 0.7	82.2 +/- 0.7
$^{171}Lu^g$	26	0.906 +/- 0.011	0.690 +/- 0.007	91.8 +/- 1.1	90.8 +/- 1.1
^{170}Hf	27	0.968 +/- 0.015	0.723 +/- 0.014	101.8 +/- 1.7	97.2 +/- 2.0
$^{169}Lu^g$	28	0.996 +/- 0.017	0.718 +/- 0.022	105.0 +/- 1.8	96.6 +/- 3.2
^{167}Tm	30	1.039 +/- 0.008	0.779 +/- 0.006	110.1 +/- 0.8	107.2 +/- 0.8
^{166}Yb	31		0.806 +/- 0.020		113.3 +/- 3.0
^{165}Tm	32		0.801 +/- 0.009		112.7 +/- 1.3
^{160}Er	37	1.131 +/- 0.031	0.903 +/- 0.017	127.4 +/- 3.7	139.4 +/- 2.9
^{161}Er	36	1.168 +/- 0.028		133.9 +/- 3.5	
^{157}Dy	40	1.282 +/- 0.017		150.9 +/- 2.1	
^{155}Dy	42	1.289 +/- 0.017		154.9 +/- 2.1	
^{155}Tb	42		0.975 +/- 0.011		156.7 +/- 1.8
^{153}Tb	44		0.985 +/- 0.015		162.8 +/- 2.6
^{152}Dy	45	1.316 +/- 0.071		164.1 +/- 9.0	
^{149}Gd	48	1.357 +/- 0.021	1.006 +/- 0.007	170.4 +/- 2.7	170.8 +/- 1.3
^{147}Gd	50		0.992 +/- 0.012		175.7 +/- 2.2
^{131}Ba	66		1.32 +/- 0.22		314. +/- 64.

1) $\Delta A = A_{target} - A_{fragment}$

2) Systematic uncertainties due to uncertainties in the range-energy relations of Northcliffe and Schilling[31]) are not included.

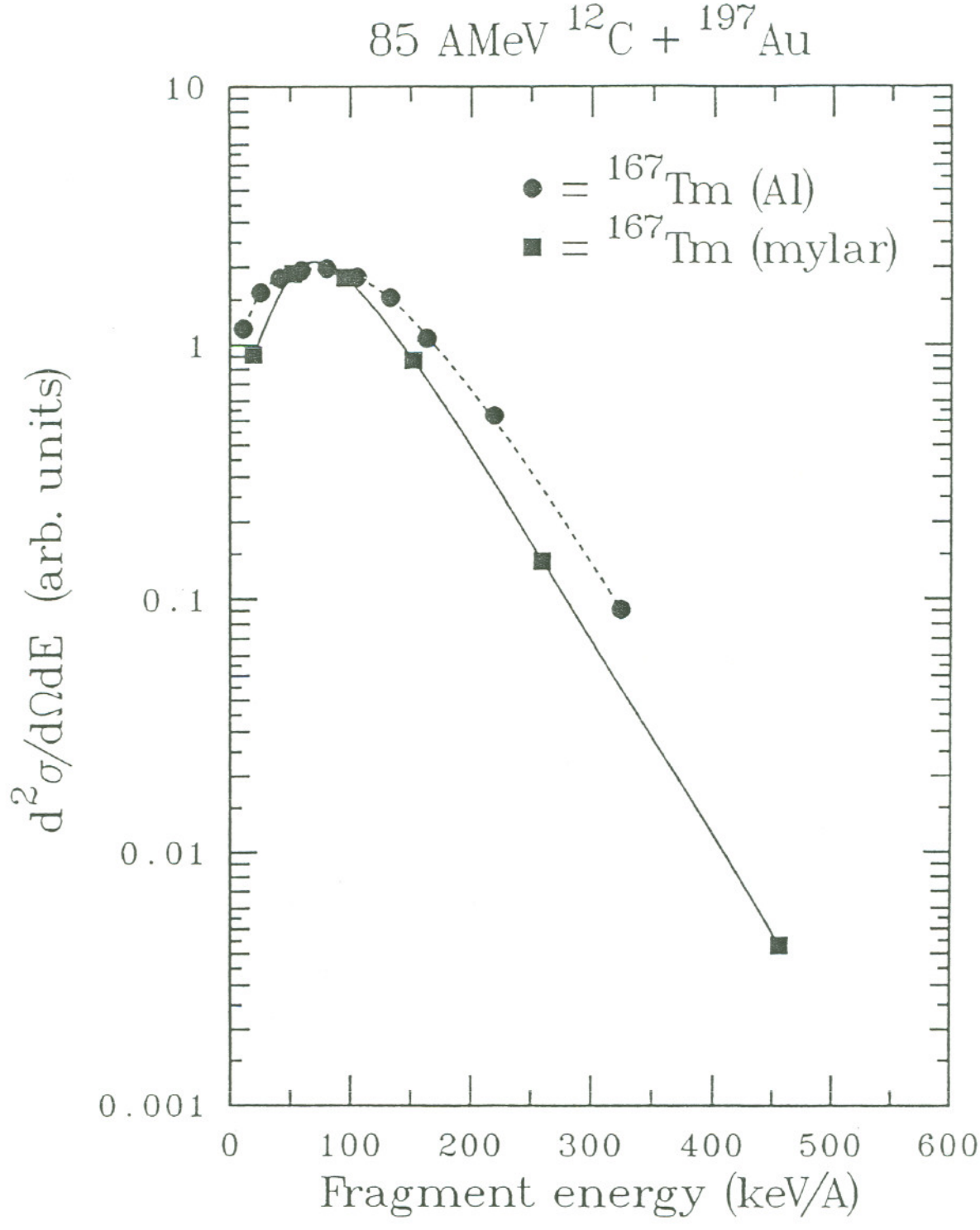

Figure 9. Comparison of the deduced ^{167}Tm energy spectra from the mylar and aluminum differential range measurements.

aluminum "detector" relative to the mylar "detector." This is consistent with the ratio of (ρ_{Al}/ρ_{mylar}) of 1.34 calculated from equation 3.

B. Comparison of Data with Previous Measurements

The mean momenta of the heavy residues can be calculated from the mean fragment energies deduced in this work. Normally, these observed momenta, $\vec{p}_{obs}$, can be understood as the vector sum of a longitudinal component, $\vec{p}_{||}$, resulting from the initial projectile-target interaction, and an isotropic component, $\vec{p}_{rms}$, resulting from the sequential evaporation of particles during fragment de-excitation, where

$$\vec{p}_{obs} = \vec{p}_{||} + \vec{p}_{rms} \qquad (4)$$

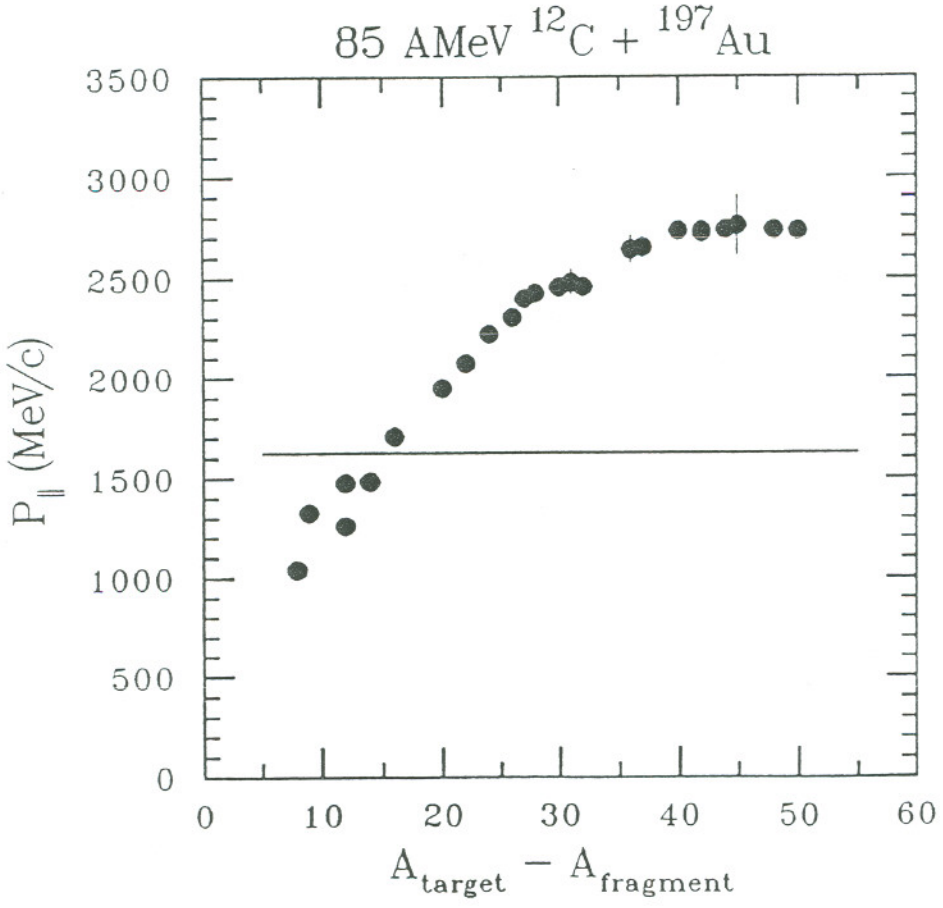

Figure 10. Deduced values of the heavy residue longitudinal momenta as a function of mass loss, ΔA, in the collision. The solid line shows the longitudinal momenta deduced for events leading to fission[15]).

A simple analysis of the vector triangle represented by equation (4) for the case where one is observing the fragments at a small fixed angle with respect to the incident beam direction shows the effect of sequential particle emission, p_{rms}, in the forward and backward direction cancels. Solution of the resulting problem leads to the deduced values of $p_{||}$ shown in Figure 10. Also shown in Figure 10 as a horizontal line is the mean value of $p_{||}$ deduced from fission fragment folding angle measurements[15]) ($\langle p_{||} \rangle / p_{cn} = 0.34$). The longitudinal momentum transfer in the nucleus-nucleus collision leading to heavy residue formation is a function of ΔA (which presumably reflects impact parameter). If one remembers that the yields of small ΔA fragments are far greater than the yields of larger ΔA fragments, then one concludes the primary target-like reaction products that survive to yield heavy residues were the result of more peripheral collisions than the target-like products that fission. Using the values of $p_{||}$ shown in Figure 10 and the isobaric yield distribution in ref.[10]) to form a proper mass-yield weighted average of $p_{||}$ for heavy residues, gives $\langle p_{||} \rangle$ = 1300 MeV/c ($\langle p_{||} \rangle / p_{cn} = 0.27$).

No evidence is seen in any of the distributions for the occurrence of a "central" collision peak (E_{res} ~ 1 MeV/nucleon) in the residue spectra as seen[11]) in the interaction of 86 MeV/nucleon ^{12}C with ^{89}Y although such a peak would have been clearly visible in the mylar catcher foil distributions.

C. Significance of the Data for Heavy Residue Measurements

Even though one is observing only the most energetic heavy residues in our forward angle differential range "detector", the deduced mean fragment energies are very low. The values range from 15 keV/nucleon (A=189) to 314 keV/nucleon (A=131) with an arithmetic average of 138 keV/nucleon. But such an average is misleading because the measured isobaric yield distribution[10]) for the reaction of 85 MeV/nucleon ^{12}C with ^{197}Au shows a factor of 50 decrease in yield as the fragment mass number decreases from 196 to 131. To make an appropriate estimate of the true mass yield weighted average residue energy would require the measurement of spectra for residues with ΔA ($=A_{target}-A_{residue}$) < 8. These residues were not seen in our forward angle "detector". Thus one can regard the mean fragment energy of 138 keV/nucleon to be an upper limit for the mean heavy residue energy.

Several groups have attempted to measure the heavy residues produced in intermediate energy nuclear collisions using various devices, such as time-of-flight spectrometers,[5,34]) etc. Frequently such detectors have low energy cutoffs below which fragments are not detected.

In Figure 11, we show the effect of various low energy cutoffs (expressed as mg/cm^2 Al) upon the fraction of the heavy residues detected (based upon our observed heavy residue spectra). Note that these fractions shown in Figure 11 are upper limits for the fraction detected because our spectra are biased towards higher energies due to observation at a forward angle. A typical low energy cutoff in a time-of-flight apparatus is a velocity of ~0.5 cm/ns which corresponds to a cutoff of ~1.2 mg/cm^2 of aluminum. Thus, in such experiments, only 60% of the A=150 fragments and ~0% of the A=180 fragments are detected, leading to a very non-representative sample of the heavy residues. For example, radiochemical measurements[42]) (which do not have a low energy threshold) of the heavy residue yields in the interaction of 32 MeV/nucleon ^{40}Ar with ^{197}Au gave a heavy residue production cross section of 2790 mb while a similar measurement[5]) using a time-of-flight spectrometer with a 0.5 cm/ns cutoff gave a cross section of 315 mb.

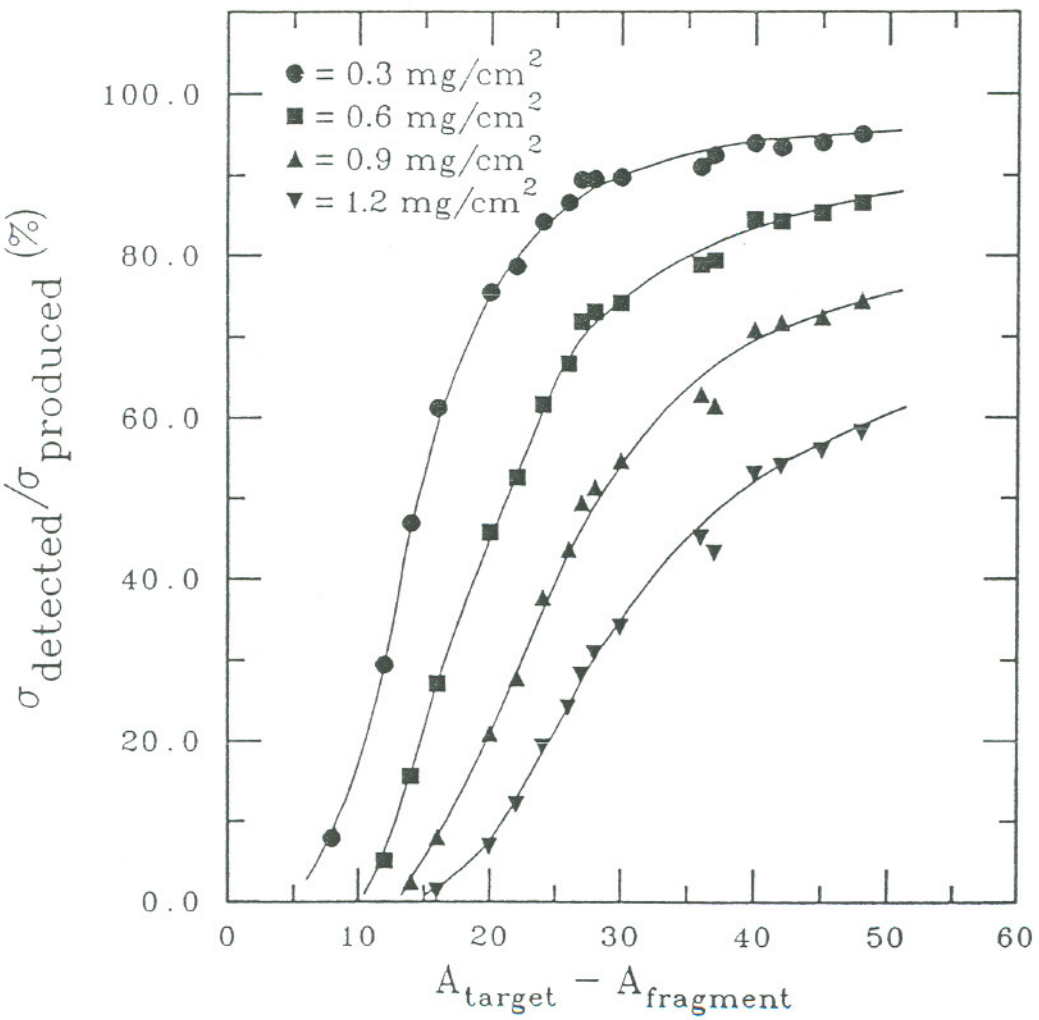

Figure 11. Effect of various low energy spectral cutoffs (expressed as mg/cm^2 Al) on the fraction of heavy residues detected.

D. Comparison of Data to Theory

The essential physics behind the heavy residue recoil properties in intermediate energy collisions was pointed out by Bondorf, et al[35]. In their statistical model, the recoil of the heavy residue is calculated by considering the number of projectile nucleons absorbed by the target nucleus and their momentum distribution (i.e., that of a dilute Boltzmann gas). The mean values of $p_{||}$ calculated[36]) in their model are compared to our data in Figure 12. Good agreement between the calculated and measured values of $p_{||}$ is seen as well as a correct prediction of the general dependence of $p_{||}$ upon ΔA. Within the Bondorf, et al. model, it is possible to uniquely associate a given impact parameter with a given ΔA value. This association and the apparent

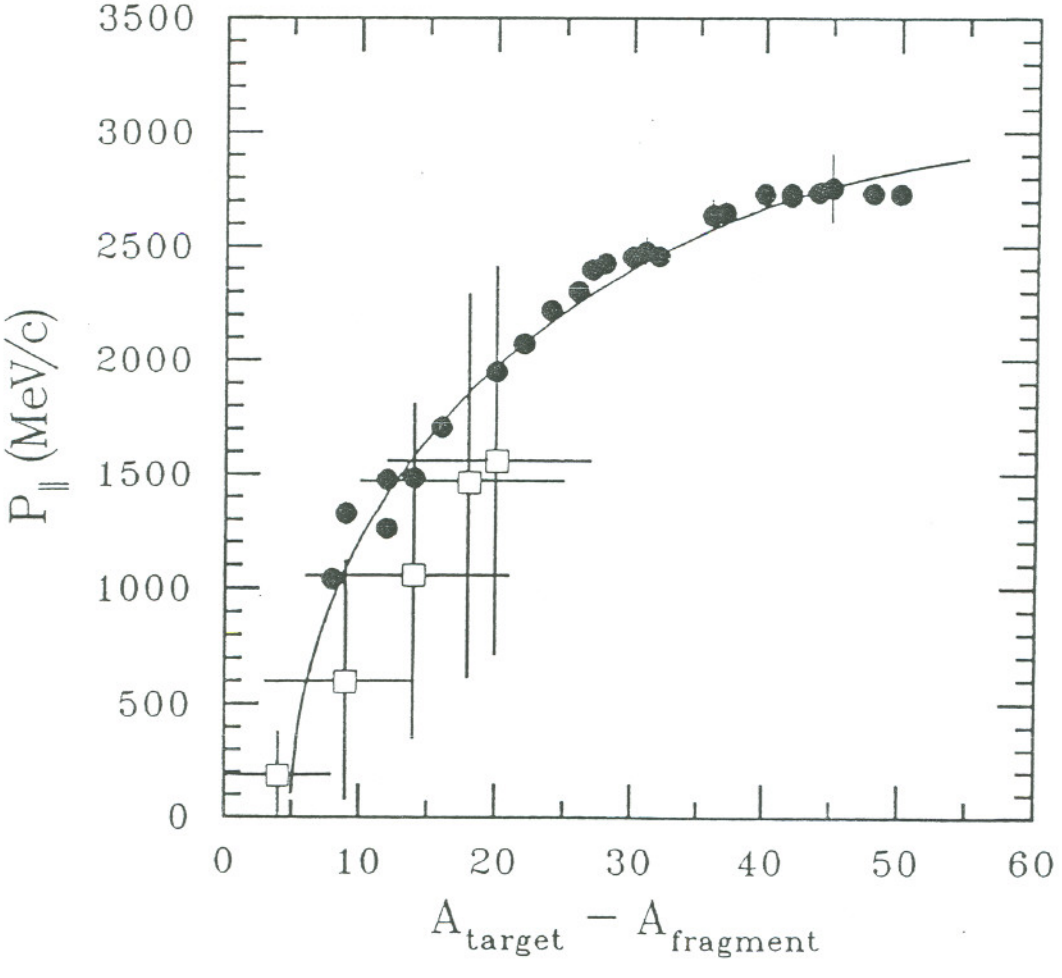

Figure 12. Comparison of the deduced values of $p_{||}$ (this work) and those calculated by Bondorf et al.[35]). The solid line represents the same empirical fit to the mean fragment energies shown in Figure 10..

validity of these calculations of mean values of $p_{||}$ would indicate the simultaneous observation of the recoil mass and energy can serve to fix the impact parameter of a intermediate energy nucleus-nucleus collision.

Despite the success of the Bondorf, et al. model (and an extended version of it[37]) in predicting the mean recoil properties of the heavy residues, the distributions of the energy and angle of emission are not given correctly[38]). It would appear that a more detailed treatment, based upon the essential ideas of the Bondorf, et al. model is needed.

In recent years, considerable success has been achieved in describing intermediate energy collisions using the quantum statistical approach of solving the Boltzmann-Uehling-Uhlenbeck equation[19,39]). This equation describes the reaction in terms of a mean field and the effect of nucleon-nucleon collisions which obey the Pauli principle. We thought it would be both interesting and important to compare the prediction of this equation with our observations of heavy residue properties.

For our calculations, we used the numerical methods of Stöcker et al.[39], known as the VUU approach. We adapted a program furnished to us by H. Stöcker to run on the CRAY supercomputers of the NMFECC at the Lawrence Livermore Laboratory. Due to limitations on the amount of computer time available to us and our desire to get immediate results to compare with experimental data, we did 90 simulations of the 85 MeV/nucleon ^{12}C + ^{197}Au reaction at a single value of the impact parameter, b = 6.05 fm, which is a representative impact parameter for this reaction. We followed each reaction for 150 fm/c using time steps in the calculation of 1.5 fm/c.

Because of the semiclassical nature of the VUU calculation, it is possible to follow the position of each nucleon in six-dimensional phase space. Since we were interested in the fate of the target-like fragment, we wrote a series of routines that identify such clusters and compute their Z and A. We calculated the total linear momentum $\vec{p}_t$ of the heavy residue as

$$\vec{p}_t = \sum_{i=1}^{A_T'} \vec{p}_i \qquad (5)$$

where the sum is carried out over all particles in the target-like fragment. The total angular momentum was calculated by using the following expression

$$\vec{J}_T = \sum_{i=1}^{A_T'} \vec{r}_i \times \vec{p}_i \qquad (6)$$

where again, the sum is carried out over the set described above. The heavy residue kinetic energy is estimated from the total linear momentum as

$$\varepsilon = \frac{p_T^2}{2M} \qquad (7)$$

where M is the mass of the heavy residue. The heavy target residue was identified as the largest cluster of original target nucleons within a spatial radius of $2r_o A_t^{1/3}$ and a momentum radius of 400 MeV/c, where r_o = 1.2 fm. The fragment excitation energy was calculated from the following expression:

$$\varepsilon^* = \left[\sum_{i=1}^{A_T'} \varepsilon_i \right] - \varepsilon_k - \varepsilon_F(Z,A) \qquad (8)$$

where the ε_i's are the single particle kinetic energies in the target-like fragment and ε_F is the total Fermi energy, calculated as follows:

$$\varepsilon_F(Z,A) = \frac{3}{5} C A^{-2/3} (Z^{5/3} + N^{5/3}) \qquad (9)$$

where A = Z + N and

$$C = \left(\frac{1}{2M}\right)\left(\frac{9\pi}{4}\right)^{2/3}\left(\frac{h^2}{r_o^2}\right) \qquad (10)$$

At the conclusion of the simulated primary reaction, we simulated the ordinary equilibrium decay of the primary fragments by particle emission using a modified version of the DFF code that has been described previously[40]). The results of these calculations for "representative" impact parameter events with observations of the angular distributions[14]) and energy spectra (this work) of "representative" heavy fragments (A=131). (Figure 13)

The agreement between the measured (points) and calculated (histogram) fragment properties is very impressive. To the best of our

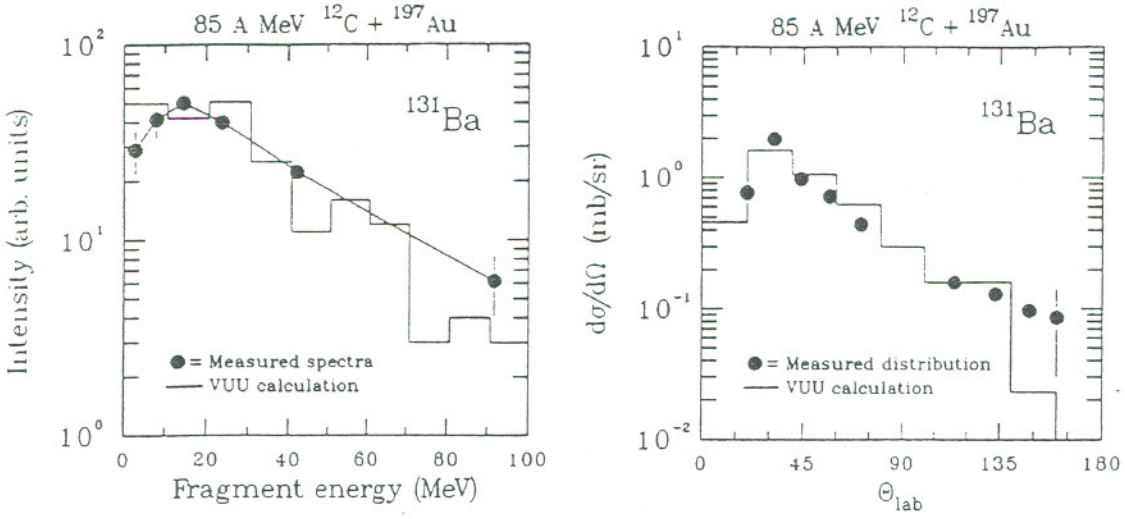

Figure 13. Comparison of calculated (histogram) and measured (solid points, line) A=131 fragment energy spectra (this work) and angular distributions[14]) for the 85 MeV/nucleon ^{12}C + ^{197}Au reaction.

knowledge, this is the first calculation of the shape of the heavy residue energy spectra for an intermediate energy reaction that is essentially correct.

IV. Summary

We have measured the heavy residue spectra for several fragments of differing Z and A from the interaction of 85 MeV/nucleon ^{12}C with ^{197}Au. The average residue energies are very low, ranging from 15 keV/nucleon (A=189) to 314 keV/nucleon (A=131). The implications of these mean energies and spectral shapes for measurements of the heavy residues have been discussed with examples of the dangers inherent in typical low velocity cutoffs in time-of-flight spectrometers. Longitudinal momenta of the heavy residues have been deduced ($\langle p_{||} \rangle / p_{cn} = 0.27$). The essential physics of heavy residue production is given by statistical models. The mean residue energies are apparently described by a simple model due to Bondorf et al.[35]) while description of the heavy residue spectral shape is given correctly by a VUU calculation.

V. Acknowledgments

We wish to thank Dupont of Sweden for providing us with the special mylar foils used in this work and the CERN health physics, ISOLDE, and accelerator personnel at the SC synchrocyclotron for their assistance during the experiment We wish to thank H. Stöcker for giving

us a copy of his VUU code. One of us (PLM) wishes to thank CERN for financial assistance during the experiment. This work was supported in part by the Swedish Natural Science Research Council, and the U.S. Department of Energy under Grant No. DE-FG06-88ER40402 and Contract No. DE-AC03-76SF00098.

References

* Present address: Universidad Simon Bolivar, Caracas, Venezuela

** Present address: Los Alamos National Laboratory, Los Alamos, NM 87545, USA

1. F. Hubert, R. Del Moral, J.P. Dufour, H. Emmerman, A. Fleury, C. Poinot, M.S. Pravikoff, H. Delagrange, and A. Lleres, Nucl. Phys. A456 (1986) 535
2. J. Blachot, J. Crancon, B. deGoncourt, A. Gizon, and A. Lleres, Z. Phys. A321 (1985) 645
3. C. Ceruti, D. Guinet, S. Chiodelli, A. Demeyer, K. Zaid, S. Leray, P. Lhenoret, C. Mazur, C. Ngo, M. Ribrag, and A. Lleres, Nucl. Phys. A453 (1986) 175
4. G. Bizard, R. Brou, H. Doubre, A. Drouet, F. Guilbault, F. Hanappe, J.M. Harasse, J.L. Laville, C. Lebrun, A. Oubahadou, J.P. Patry, J. Peter, G. Ployart, J.C. Steckmeyer, and B. Tamain, Z. Phys. A323 (1986) 459
5. G. Bizard, R. Brou, H. Doubre, A. Drouet, F. Guilbault, F. Hanappe, J.M. Harasse, J.L. Laville,C. Lebrun, A. Oubahadou, J.P. Patry, J. Peter, G. Ployart, J.C. Steckmeyer, and B. Tamain, Nucl. Phys. A456 (1986) 173.
6. M.F. Rivet, B. Borderie, H. Gauvin, D. Gardes, C. Cabot, F. Hanappe, and J. Peter, Phys. Rev. C34 (1986) 1282.
7. E.C. Pollaco, M. Conjeaud, S. Harar, C. Volant, Y. Cassagnou, R. Dayras, R. Legrain, M.S. Nguyen, H. Oeschler, and F. Saint-Laurent, Phys. Lett. 146B (1984) 29.
8. J.P. Dufour, H. Delagrange, R. Del Moral, A. Fleury, F. Hubert, Y. Llabador, M.B. Mauhourat, K.H. Schmidt, and A. Lleres, Nucl. Phys. A387 (1982) 157c.
9. D. Molzahn, T. Lund, R. Brandt, E. Hagebø, I.R. Haldorsen, and C.R. Serre, J. Radioanal. Chem. 80 (1983) 109.
10. W. Loveland, K. Aleklett, P.L. McGaughey, K.J. Moody, R.M. McFarland, R.H. Kraus, Jr., and G.T. Seaborg, Lawrence Berkeley Laboratory Report LBL-16280,July, 1983.
11. A. Lleres, J. Blachot, J. Crancon, A. Gizon, and H. Nifenecker, Z. Phys. A312 (1983) 177.
12. B. Grabez, R. Beckmann, P. Vater, and R. Brandt, Phys. Lett. B184 (1987) 144.
13. B. Grabez, R. Beckmann, P. Vater, and R. Brandt, Phys. Rev. C34 (1986) 170.
14. R.H. Kraus, Jr., W. Loveland, K. Aleklett, P.L. McGaughey, T.T. Sugihara, G.T. Seaborg, T. Lund, Y. Morita, E. Hagebø and I.R. Haldorsen, Nucl. Phys. A432, (1985) 525.
15. U. Lynen, H. Ho, W. Kuhn, D. Pelte, U. Winkler, W.F.J. Müller, Y.T. Chu, P. Doll, A. Gobbi, K. Hildenbrand, A. Olmi, H. Sann, H. Stelzer, R. Bock, H. Löhner, R. Glashow, and R. Santo, Nucl. Phys. A387 (1982) 129c.

16. M.F. Rivet, B. Borderie, S. Song, D. Guerreau, H. Oeschler, R. Bimbot, I. Forest, J. Galin, D. Gardes, B. Gatty, M. Lefort, B. Tamain, and X. Tarrago, Nucl. Phys. A387 (1982) 143c.

17. J. Galin, H. Oeschler, S. Song, B. Borderie, M.F. Rivet, I. Forest, R. Bimbot, D. Gardes, B. Gatty, H. Guillemot, M. Lefort, B. Tamain, and X. Tarrago, Phys. Rev. Lett. 48 (1982) 1787.

18. H.A. Khan, T. Lund, P. Vater, R. Brandt, and J.W.N. Tuyn, Phys. Rev. C28 (1983) 1630.

19. J. Aichelin and G. Bertsch, Phys. Rev. C31 (1985) 1730.

20. J. Aichelin and H. Stöcker, Phys. Lett. 163B (1985) 59.

21. J. Aichelin, Nucl. Phys. A447 (1985) 569c.

22. J. Aichelin, Phys. Rev. C33 (1986) 537.

23. J. Aichelin, J. de Physique, C4 (1986) C4-63.

24. H.H. Gan, S.J. Lee and S. Das Gupta, Phys. Rev. C36 (1987) 2365.

25. W. Loveland, K. Aleklett, L. Sihver, Z. Xu, C. Casey, and G.T. Seaborg, Nucl. Phys. A471 (1987) 175c.

26. K. Aleklett (to be published)

27. D.J. Morrissey, D. Lee, R.J. Otto, and G.T. Seaborg, Nucl. Instr. Meth. 158 (1978) 499.

28. K. Aleklett, Radiochemist's Gamma Ray Table, 2nd Ed., (OSU, 1987)

29. U. Reus, and W. Westmeier, At. Data and Nucl. Data Tables 29(1983)1.

30. L. Winsberg, Phys. Rev. 135 (1964) B1105.

31. L.C. Northcliffe amd R.F. Schilling, Nucl. Data Tables, A7 (1970) 233.

32. L. Winsberg and J.M. Alexander, Phys. Rev. 121 (1961) 518.

33. J. Lindhard, M. Scharff, and J. Schiøtt, Kgl. Danske Videnskab. Selskab Matt. Fys. Medd. 33, No. 14 (1963)

34. M.F. Rivet, B. Borderie, H. Gauvin, D. Gardes, C. Chabot, F. Hanappe, and J. Peter, Phys. Rev. C34 (1986) 1282.

35. J.P. Bondorf, J.N. De, G. Fai, and A.O.T. Karvinen, Nucl. Phys. A430 (1984) 445.

36. The calculations shown in Figure 11 are for the 85 MeV/nucleon ^{12}C + ^{108}Ag reaction presented in terms of the mass loss ΔA. For very peripheral collisions, the dependence of the calculated quantities on target nucleus mass number is expected to be weak.

37. D. Bandopadhyay, S.K. Samaddar, K. Krishan, and J.N. De, GANIL Report P. 87-14.

38. Comparison of the angular distributions calculated in ref. 37 and the measured distributions(ref. 14) shows significant differences.

39. H. Kruse, B.V. Jacak, J.J. Molitoris, G.D. Westfall, and H. Stöcker, Phys. Rev. C31 (1985) 1770.

40. P.L. McGaughey, W. Loveland, D.J. Morrissey, K. Aleklett,and G.T. Seaborg, Phys. Rev. C31 (1985) 896.

41. T. Sikkeland, Phys. Rev. 135 (1964) B669.

42. K. Aleklett, W. Loveland, L. Sihver, Z. Xu, C. Casey, D.J. Morrissey, J.O. Liljenzin, M. de Saint-Simon, and G.T. Seaborg, Phys. Rev C (submitted for publication)

43. H. Kudo, K.J. Moody, and G.T. Seaborg, Phys. Rev. C30 (1984) 1561

44. K. Aleklett, W. Loveland, C. Casey, D.J. Morrissey, J.O. Liljenzin, M. de Saint-Simon, L.Sihver, and G.T. Seaborg, (in preparation)